Journal of Peptide Science
J. Pept. Sci. 2008; **14**: 342–348
Published online 16 November 2007 in Wiley InterScience (www.interscience.wiley.com). DOI: 10.1002/psc.943

JOURNAL OF PEPTIDE SCIENCE

The structural and functional contribution of *N*-terminal region and His-47 on Taiwan cobra phospholipase A_2

PEI-HSIU KAO,[a] KU-CHUNG CHEN,[a] SHINNE-REN LIN[b] and LONG-SEN CHANG[a]*

[a] Institute of Biomedical Sciences, National Sun Yat-Sen University-Kaohsiung Medical University Joint Research Center, National Sun Yat-Sen University, Kaohsiung 804, Taiwan
[b] Department of Medicinal and Applied Chemistry, Kaohsiung Medical University, Kaohsiung 807, Taiwan

Received 15 July 2007; Revised 23 August 2007; Accepted 28 August 2007

Abstract: Modification of His-47 and removal of the *N*-terminal octapeptide caused a different effect on the structure of *Naja naja atra* (Taiwan cobra) phospholipase A_2 (PLA_2). Unlike native enzyme, Ca^{2+} induced an alteration in the structural flexibility of His-modified PLA_2. Moreover, the spatial positions of Trp residues in His-modified PLA_2 were not properly rearranged toward lipid–water interface in the presence of Ca^{2+}. CD spectra and fluorescence measurement showed that the dynamic properties of Trp residues and the gross conformation of *N*-terminally truncated PLA_2 were totally different from native enzyme. Although a precipitous drop in the enzymatic activity was observed with modified PLA_2, His-modified PLA_2 and *N*-terminally truncated PLA_2 retained cytotoxicity on inducing necrotic death of human neuroblastoma SK-N-SH cells. Our data suggest that structural perturbations elicited by the chemical modification cause a dissociation of enzymatic activity and cytotoxicity of PLA_2.

Keywords: phospholipase A_2; *N*-terminal truncation; histidine modification; structural perturbation

INTRODUCTION

The phospholipase A_2 (PLA_2) enzymes from snake venom and mammalian pancreas specifically catalyze the hydrolysis of fatty-acid bond at the position 2 of 1,2-diacyl-*sn*-phosphoglycerides in the presence of Ca^{2+} [1]. X-ray crystallographic analyses show that snake venom PLA_2 enzymes and pancreatic PLA_2 enzymes share a remarkable degree of structural homology [2–7], but differ in details such as the extent of secondary structure and positioning invariant side chains. The binding of PLA_2 to the surface of aggregated substrate such as membranes or micelles substantially increases the enzyme activity, an effect known as interfacial activation [8–10]. It is well-known that the *N*-terminal region of PLA_2 enzymes act as a regulatory domain that mediates interfacial activation of these enzymes [11]. Several lines of evidence show that the *N*-terminal region functionally contributes to facilitate a productive-mode orientation of PLA_2 at the membrane surface [11,12]. Moreover, an allosteric coupling between membrane-binding site and the catalytic center of PLA_2 is suggestive to regulate the interfacial activation of the enzyme [13]. Noticeably, recent studies reveal that a nontoxic porcine pancreas PLA_2 induces apoptotic cell deaths of RAW 246.7 cells in a PLA_2-activity independent manner [14]. This indicates that the interfacial activation should not involve heavily in the cytotoxicity of PLA_2 enzymes. In order to address the contribution of structural dynamics which resides with the *N*-terminal region and catalytic center to the biological activities of PLA_2, comparative studies on native and chemically modified *Naja naja atra* PLA_2 are conducted in the present study.

MATERIALS AND METHODS

PLA_2 was isolated from *N. naja atra* (Taiwan cobra) venom according to the methods previously described [15]. His-47 of PLA_2 was modified with *p*-bromophenacyl bromide (BPB) essentially according to the procedure described in Yang *et al.* [16]. After CNBr cleavage at Met-8 of PLA_2 [17], the large *C*-terminal fragment (CBII) was separated from the *N*-terminal octapeptide by HPLC on a column (4.6 mm × 25 cm) of SynChropak RP-P eluted with a linear gradient of 25–50% acetonitrile for 60 min. Acrylamide, egg yolk phosphatidylcholine (EYPC) and dimyristoyl phosphatidic acid (DMPA) were purchased from Sigma-Aldrich Inc., and SynChropak RP-P column (4.6 mm × 25 cm) was obtained from SynChrom Inc. (Lafayette, IN, USA). Cell culture supplies were purchased from GIBCO/Life Technologies Inc. Unless otherwise specified, all other reagents were of analytical grade.

PREPARATION OF LIPOSOMES

EYPC/DMPA was dissolved in chloroform/methanol (v/v, 2:1) at a molar ratio of 9:1 and dried by evaporation. Buffer (10 mM Tris-HCl-100 mM NaCl, pH 7.5) was added to the film of lipids, and the suspension was shaken vigorously after hydration. The multilamellar vesicles obtained in this way were

*Correspondence to: Long-Sen Chang, Institute of Biomedical Sciences, National Sun Yat-Sen University, Kaohsiung 804, Taiwan; e-mail: lschang@mail.nsysu.edu.tw

extruded 10 times, above the transition temperature through a 100 nm polycarbonate filter.

TIME-RESOLVED FLUORESCENCE MEASUREMENT

Time-resolved fluorescence spectroscopy was performed using the technique of time-correlated single photon counting. The samples were measured in an Edinburgh Instruments OB920 spectrometer equipped with TCC900 photon counting electronics. The excitation pulses were at 295 nm, and the emission was collected at 350 nm. Discrete component analysis was performed with F900 software (Edinburgh Instruments) employing a nonlinear least-squares procedure. The decays were fitted by a two- or three-exponential decay function. The quality of the fit was determined by the value of the reduced chi-squared statistical parameter and by visual inspection of residues. In all cases, the χ^2 values were close to 1.0, and the weighted residues as well as the autocorrelation of the residues were randomly distributed around zero, indicating an optimal fit. Each reported lifetime (τ) was obtained from the average of three measurements, with the scatter being <10%. The fraction intensities (fi) were calculated from the values of lifetimes (τi) and pre-exponential factors (αi) as follows: $f\mathrm{i} = \alpha\mathrm{i}\tau\mathrm{i}/\sum\alpha\mathrm{i}\tau\mathrm{i}$.

CELL VIABILITY ASSAYS

Human neuroblastoma SK-N-SH cells were cultured with Dulbecco's modified Eagle's medium containing 10% fetal calf serum, 2 mM glutamine and penicillin/streptomycin (100 μg/ml) in a humidified 95% air, 5% CO_2 incubator. Exponentially growing cells (1×10^5) were plated in 96-well plates and after 24 h of growth treated with a series of concentrations of native and modified PLA_2 in serum free medium. At suitable time intervals, MTT solution was added to each well at a final concentration of 0.5 mg/ml and incubated for 4 h. Formazan crystals resulting from MTT reduction were dissolved by addition of 100 μl DMSO per well. The absorbance was detected at 595 nm using a plate reader.

DETECTION OF APOPTOTIC CELLS

Annexin V/propidium iodide staining was carried out according to the manufacturer's protocol (annexin V-FITC kit from Molecular Probes). After PLA_2 treatment at indicated time, the SK-N-SH cells were washed with cold PBS and resuspended with binding buffer (10 mM HEPES, pH 7.4, 140 mM NaCl, 2.5 mM $CaCl_2$) before transferring 1×10^5 cells to a 5 ml tube. Then 5 μl each of annexin V-FITC and propidium iodide were added, and the cells were incubated for 15 min in the dark. Binding buffer (400 μl) was then added to each tube and analyzed by a Beckman Coulter Epics XL flow cytometer.

OTHER TESTS

Determination of PLA_2 activity, fluorescence measurement, fluorescence quenching studies and CD measurement were performed in essentially the same manner as previously described [18–20]. Statistical analyses were determined using the unpaired Student's t-test. A value of $P < 0.05$ was accepted as an indication of statistical significance.

RESULTS

N. naja atra PLA_2 contains three Trp residues at positions 18, 19 and 61. Mutagenesis studies show that the three Trp residues are located at lipid–water interface for catalytic action [21]. Thus, the Trp fluorescence can trace an alteration in the structural dynamics of PLA_2 for performing enzymatic activity. As shown in Figure 1, the intrinsic fluorescence of PLA_2 markedly decreased after removal of the *N*-terminal octapeptide (CBII) or modification of His-47 (BPB-PLA_2). These suggest an alteration in the microenvironment of Trp residues of the modified PLA_2 compared with native enzyme.

As shown in Figure 2(A), the fluorescence decay of PLA_2 was dominated by short- (0.14 ns), intermediate- (1.94 ns) and long-lived (3.81 ns) components that contributed 21.1, 36.8 and 42.1% of the total fluorescence intensity, respectively. The Trp fluorescence lifetime of bromophenacylated PLA_2 (BPB-PLA_2) comprised three components at 0.07 (short-lived), 1.76 (intermediate-lived) and 3.39 (long-lived), respectively (Figure 2(B)).

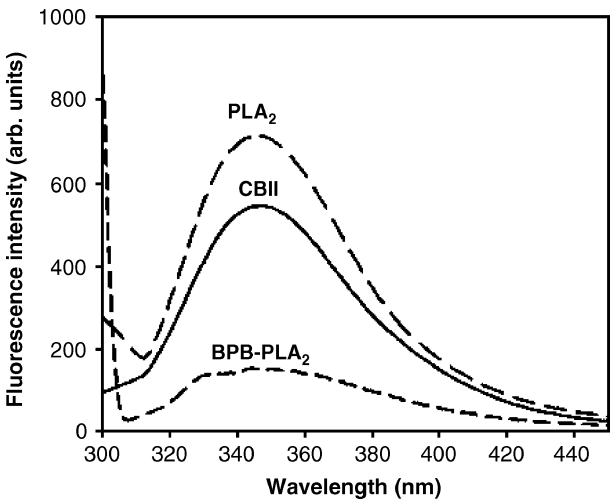

Figure 1 Fluorescence spectra of native and modified PLA_2 at an excitating wavelength of 295 nm.

DOI: 10.1002/psc

The contribution of the short-, intermediate- and long-lived component to the total fluorescence was 38.3, 52.6 and 9.1%, respectively. Alternatively, the Trp fluorescence emission decay of CBII was dominated by short- (0.17 ns), intermediate- (1.75 ns) and long-lived (4.68 ns) components that contributed 30.6, 38.4 and 31.0% of the total fluorescence intensity, respectively (Figure 2(C)). These observations again emphasize that the microenvironment of Trp residues in PLA_2 is perturbed by removal of *N*-terminal region and modification of His-47.

Acrylamide quenching has been used to assess the degree of exposure of Trp residues in proteins [22]. Quenching of Trp residues is analyzed by the Stern–Volmer equation: $Fo/F = 1 + Kq[Q]$, where Fo and F are the fluorescence intensities at an appropriate emission wavelength in the absence and presence of acrylamide, Kq is the collisional quenching constant, and $[Q]$ is the concentration of acrylamide. As shown in Figure 3, the linearity of Stern–Volmer plots for PLA_2 indicated an equal accessibility of Trp-18, Trp-19 and Trp-61 for acrylamide. However, the difference in the degree of exposure of Trp residues was observed between Ca^{2+}-bound PLA_2 and metal-free PLA_2. This reflects that Ca^{2+} induces a conformational change of PLA_2 accompanied by the altering of the spatial positions of Trp residues. Removal of *N*-terminal region and modification of His-47 caused a marked decrease in the accessibility of Trp residues for acrylamide. Moreover, the degree of exposure of Trp residues in the modified PLA_2 was insignificantly changed by the binding of Ca^{2+}.

As shown in Figure 4(C), CD spectra revealed that the secondary structure of PLA_2 was dominated with α-helix, and the gross conformation of PLA_2 changed upon binding with Ca^{2+}. The conformation of PLA_2,

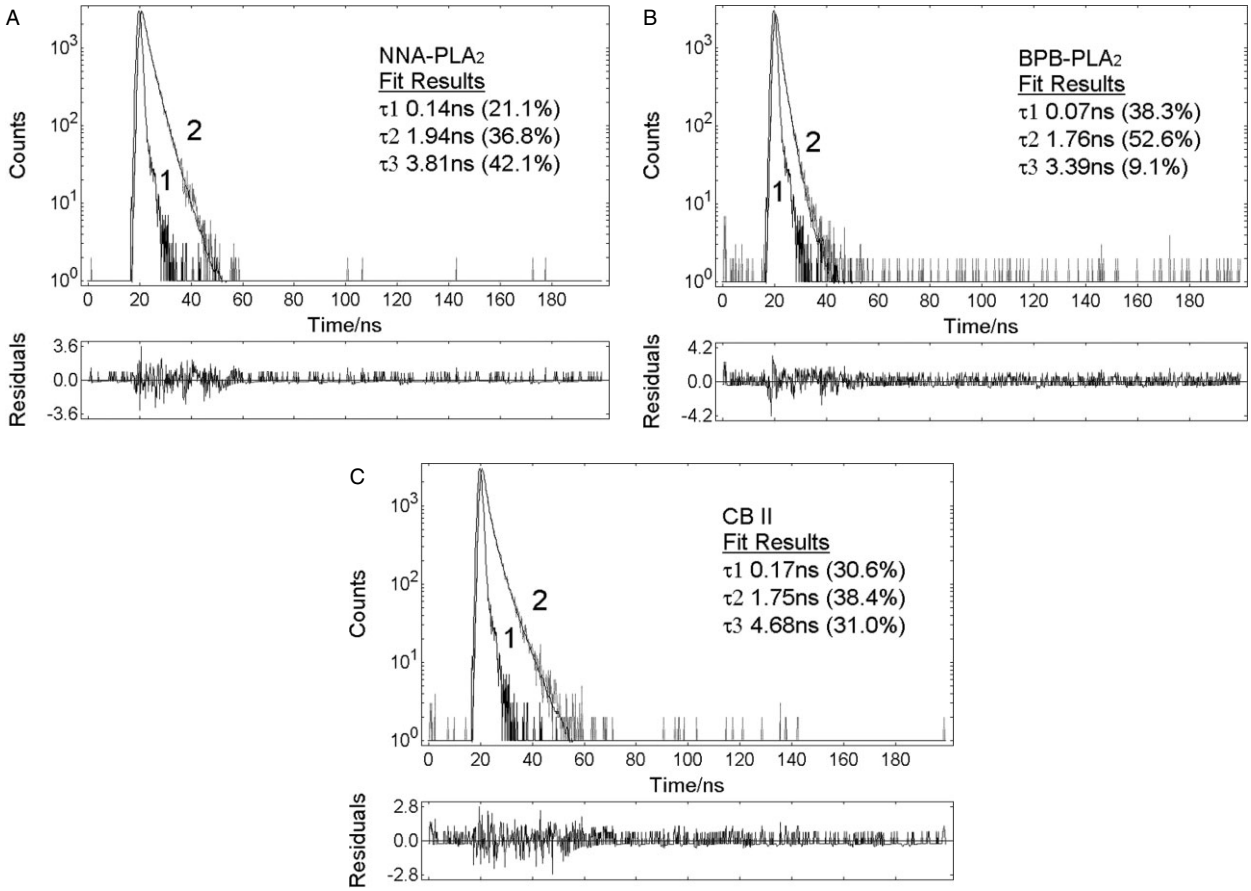

Figure 2 Trp fluorescence decay curve of native and modified PLA_2. (A) Trp fluorescence decay curve of PLA_2. The excitation and emission wavelength are 295 and 350 nm, respectively. The sample cuvette contained 3.6 μM PLA_2. Curve 1, Instrumental response function; Curve 2, Superposition of the observed decay and fitted curve. Distribution of the residues shown below the plot is the difference between the observed data and the best-fit curve. (B) Trp fluorescence decay curve of BPB-PLA_2. The excitation and emission wavelength are 295 and 350 nm, respectively. The sample cuvette contained 3.6 μM BPB-PLA_2. Curve 1, Instrumental response function; Curve 2, Superposition of the observed decay and fitted curve. Distribution of the residues shown below the plot is the difference between the observed data and the best-fit curve. (C) Trp fluorescence decay curve of CBII. The excitation and emission wavelength are 295 and 350 nm, respectively. The sample cuvette contained 3.6 μM CBII. Curve 1, Instrumental response function; Curve 2, Superposition of the observed decay and fitted curve. Distribution of the residues shown below the plot is the difference between the observed data and the best-fit curve.

DOI: 10.1002/psc

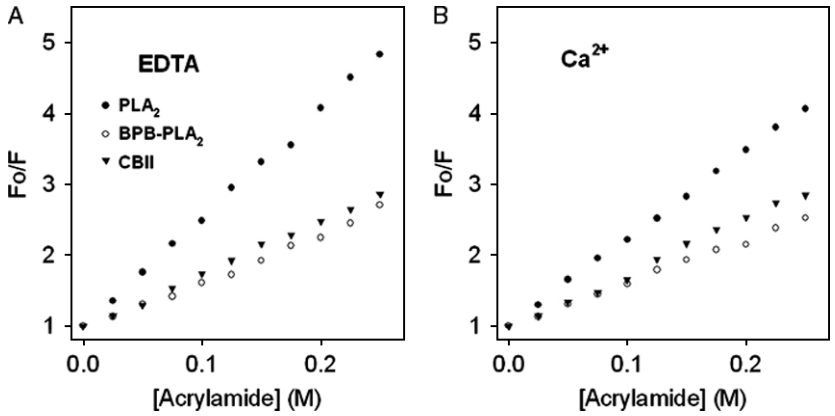

Figure 3 Stern–Volmer plots for acrylamide quenching of Trp fluorescence of native and modified PLA_2. Native and modified PLA_2 (0.05 mg/ml) in 10 mM Tris-100 mM NaCl (pH 8.0) were quenched by acrylamide in the presence of (A) 1 mM EDTA or (B) 1 mM Ca^{2+}.

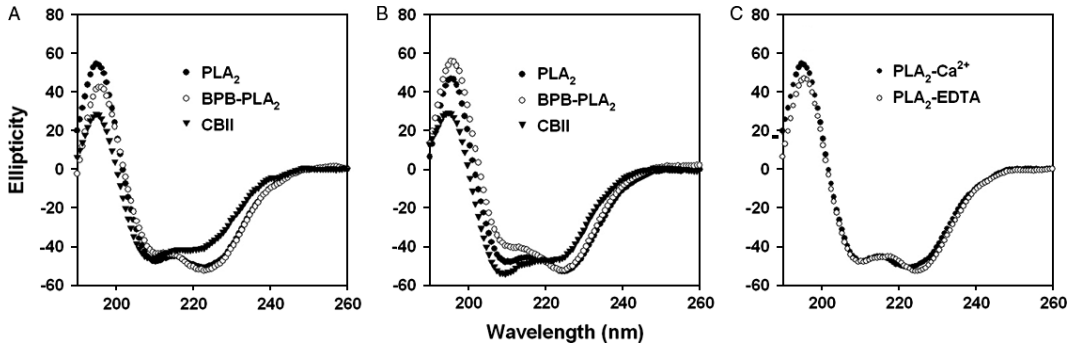

Figure 4 CD spectra of native and modified PLA_2. The CD spectra were measured at a protein concentration of 1 mg/ml in 10 mM Tris-100 mM NaCl (pH 8.0) containing (A) 1 mM Ca^{2+} or (B) 1 mM EDTA. (C) The CD-spectra of Ca^{2+}-bound and metal-free PLA_2. CD spectra were obtained on a Jasco J-810 spectropolarimeter with a cell path-length of 0.5 mm. The CD spectra were measured from 260 to 190 nm, and CD spectra were obtained by averaging the signals of five scans.

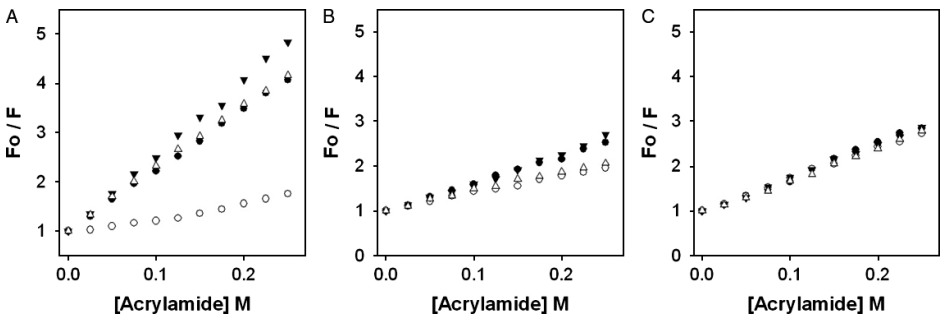

Figure 5 Effect of phospholipid vesicles on acrylamide quenching of native and modified PLA_2. Protein (0.05 mg/ml) was dissolved in 10 mM Tris-100 mM NaCl (pH 8.0) containing 1 mM Ca^{2+} (●, ○) or 1 mM EDTA (▼, Δ). Quenching of Trp fluorescence of (A) PLA_2, (B) BPB-PLA_2 and (C) CBII were carried out in the absence (●, ▼) or presence (○, Δ) of 160 μM EYPC/DMPA liposome, respectively. The excitating wavelength was 295 nm, and the fluorescence intensity was monitored at 350 nm.

CBII and BPB-PLA_2 differed either in the absence or presence of Ca^{2+} (Figure 4(A) and (B)). The ellipticity ratio $[\theta]_{223}/[\theta]_{209}$ is known to increase with increasing flexibility of the helices [23,24]. Thus, the structural flexibility of BPB-PLA_2 was higher than CBII and PLA_2 in a metal-free buffer (Figure 4(B)), while the structural flexibility of BPB-PLA_2 decreased upon binding with Ca^{2+}. Moreover, the finding that Ca^{2+}-binding altered the CD spectra of BPB-PLA_2 and CBII implicated that the Ca^{2+}-binding ability of BPB-PLA_2 and CBII was not impaired.

As shown in Figure 5(A), compared with metal-free PLA_2, the degree of exposure of Trp residues in Ca^{2+}-bound PLA_2 was notably decreased by binding

DOI: 10.1002/psc

with phospholipids. This reflects that Ca^{2+}-bound PLA_2 adopts an active conformation in which Trp residues shift to the lipid-water interface and thus become less accessible for acrylamide. Upon binding with phospholipids, the change in the accessibility of Trp residues for acrylamide insignificantly differed between Ca^{2+}-bound BPB-PLA_2 and metal-free BPB-PLA_2. Unlike that noted with PLA_2 and BPB-PLA_2, quenching of CBII was not significantly affected by the addition of phospholipid vesicles. These results indicate that the fine structure neighboring Trp residues of Ca^{2+}-bound PLA_2 is distinct from that of Ca^{2+}-bound BPB-PLA_2 and Ca^{2+}-bound CBII.

As shown in Figure 6(A), the cytotoxic effect of PLA_2, BPB-PLA_2 and CBII was evaluated on SK-N-SH cells. The cell viability was decreased by approximately 40% ($P < 0.05$ *vs.* untreated control cells) after treatment with 10 μM PLA_2 for 24 h. Alternatively, compared with untreated control cells, approximately 80 and 92% viability ($P < 0.05$ *vs.* untreated control cells) were observed with the cells treated with 10 μM BPB-PLA_2 and CBII, respectively. To evaluate whether PLA_2 cytotoxicity was primarily necrotic or apoptotic, cells were stained with propidium iodide and annexin V. In the absence of PLA_2, SK-N-SH cells were viable with low PI and annexin V staining (lower left quadrants of the dot plots, Figure 6(B)). PLA_2 treatment resulted in an increase in propidium iodide staining. No evidence of annexin V staining (lower right quadrants) was detected in PLA_2-treated SK-N-SH cells, thus the cytotoxic activity of PLA_2 was necrotic and not apoptotic. Similar results were observed when SK-N-SH cells were treated with BPB-PLA_2 or CBII.

DISCUSSION

The results of the present study show that modification of His-47 and truncation at *N*-terminus differently alter the gross conformation of PLA_2 and the spatial orientation of Trp residues in response to Ca^{2+}-binding. Additionally, a complete loss of enzymatic activity is observed with the modified PLA_2 (data not shown). X-ray crystallographic analyses show that, in addition to Trp-18, the residues Leu-2, Tyr-3, Lys-6, Ile-9, Arg-30 and Tyr-68 constitute the hydrophobic channel involves in the interaction of enzyme molecule with a phospholipids/substrate [2]. Together with the findings that the intact Trp residues are essential for the enzymatic activity of *N. naja atra* PLA_2 [21,25], Ca^{2+}-induced change in the spatial positions of Trp residues and gross conformation of PLA_2 should be associated with the event for rearrangement of functional residues toward the interaction with phospholipids/substrate. Previous studies showed that modification of bovine pancreas PLA_2 and *Agkistrodon halys* PLA_2 by BPB led to conformational changes outside of the catalytic site [26,27]. Moreover, an engineered human pancreas PLA_2 lacked the *N*-terminal ten residues was found to bind to membrane with weaker affinity and at random orientation [12]. Taken together, our data suggest that modification of His-47 and removal of *N*-terminal octapeptide disable PLA_2 to have an appropriately conformational change in response to Ca^{2+}-binding. In consequence, distorted effects on productively interacting with phospholipids/substrate and catalytic activity are observed.

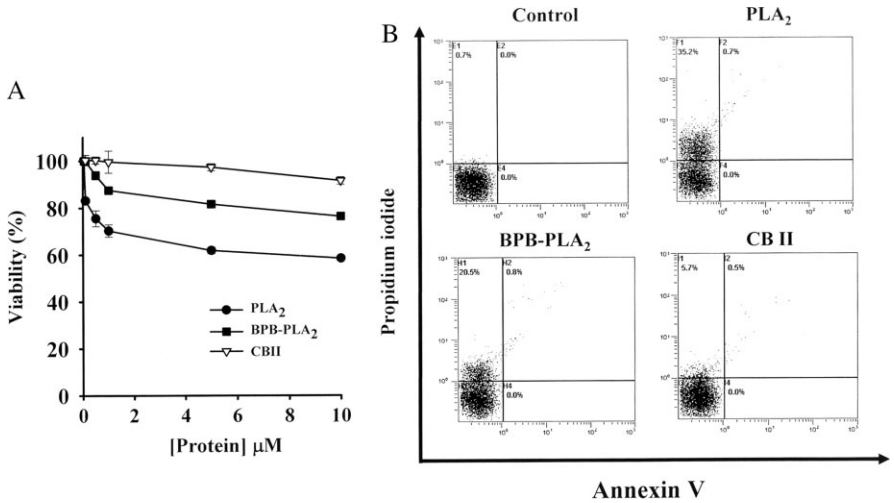

Figure 6 Native and modified PLA_2 induced necrotic death of SK-N-SH cells. (A) The cells were treated with varying concentrations of native and modified PLA_2 for 24 h, and then the cell viability was determined by MTT assay. The percentage of viable cells was calculated as a ratio of absorbance at 595 nm of treated to control cells. Data are represented mean ± SD of three independent experiments. (B) SK-N-SH cells were incubated with 10 μM native and modified PLA_2 for 24 h. Cell deaths were analyzed by dual-parameter flow cytometry utilizing FITC-conjugated annexin V and propidium iodide. On the flow cytometric scatter graphs, the left lower quadrant represents remaining live cells. The left upper quadrant represents the accumulation of necrotic cells.

DOI: 10.1002/psc

In contrast to a complete loss of the enzymatic activity ($P < 0.05$ *vs.* PLA_2), BPB-PLA_2 and CBII still retain cytotoxic effect. This indicates that the enzymatic activity is not critical for the cytotoxicity of PLA_2. It is in line with the observation that porcine pancreas PLA_2 induces apoptotic cell death without the involvement of its enzymatic activity [14]. Recently, β-bungarotoxin (a presynaptic PLA_2 neurotoxin) was found to induce apoptotic death of cultured neurons in a PLA_2 activity-independent manner, and the cytotoxicity of β-bungarotoxin was mediated by potassium channel [28]. Whether *N. naja atra* PLA_2-induced necrotic cell death is a receptor-mediated pathway still remains to be resolved. The fact that several membrane receptors for PLA_2 enzymes have been reported previously [29–32] supports this possibility. Taking into account that the conformation of BPB-PLA_2 and CBII is different from that of native PLA_2, alterations in the capability for binding with cellular targets is plausible to determine the potency of their cytotoxicity. It is worth noting that the present study does not unambiguously elucidate the structural element of *N. naja atra* PLA_2 closely relates to the cytotoxicity. Ponce-Soto *et al.* [33] proposed that a cluster of basic residues in the *C*-terminal region of PLA_2 enzymes was associated with myonecrotic effect. However, the *C*-terminus of *N. naja atra* PLA_2 lacks the cluster of the basic residues. Alternatively, studies on PLA_2 chimeras revealed that the intact *N*-terminal region of *Oxyuranus scutellatus scutellatus* PLA_2 was crucial for both enzymatic activity and pharmacological activities [34]. Taken together, the *N*-terminal region of *N. naja atra* PLA_2 is likely involved in the binding with its cellular targets. Moreover, the distorted conformation with CBII might further abrogate the cytotoxic activity of *N. naja atra* PLA_2.

Acknowledgements

This work was supported by grant NSC95-2320-B110-007-MY3 from the National Science Council, ROC (to L.S. Chang), and grant of National Sun Yat-Sen University-Kaohsiung Medical University Joint Center.

REFERENCES

1. Kini RM. Phospholipase A_2-a complex multifunctional protein puzzle. In *Venom Phospholipase A_2 Enzymes: Structure, Function and Mechanism*, Kini RM (ed.). John Wiley & Sons: Chichester, 1997; 1–28.
2. Scott DL, White SP, Otwinowski Z, Yuan W, Gelb MH, Sigler PB. Interfacial catalysis: the mechanism of phospholipase A_2. *Science* 1990; **250**: 1541–1546.
3. White SP, Scott DL, Otwinowski Z, Gelb MH, Sigler PB. Crystal structure of cobra-venom phospholipase A_2 in a complex with a transition-state analogue. *Science* 1990; **250**: 1560–1563.
4. Tang L, Zhou YC, Lin ZJ. Crystal structure of agkistrodotoxin, a phospholipase A_2-type presynaptic neurotoxin from *Agkistrodon halys pallas*. *J. Mol. Biol.* 1998; **282**: 1–11.
5. Singh G, Gourinath S, Sharma S, Paramasivam M, Srinivasan A, Singh TP. Sequence and crystal structure determination of a basic phospholipase A_2 from common krait (*Bungarus caeruleus*) at 2.4 Å resolution: identification and characterization of its pharmacological sites. *J. Mol. Biol.* 2001; **307**: 1049–1059.
6. Ambrosio AL, Nonato MC, de Araujo HS, Arni R, Ward RJ, Ownby CL, de Souza DH, Garratt RC. A molecular mechanism for Lys49-phospholipase A_2 activity based on ligand-induced conformational change. *J. Biol. Chem.* 2005; **280**: 7326–7335.
7. Murakami MT, Gabdoulkhakov A, Genov N, Cintra AC, Betzel C, Arni RK. Insights into metal ion binding in phospholipases A_2: ultra high-resolution crystal structures of an acidic phospholipase A_2 in the Ca^{2+} free and bound states. *Biochimie* 2006; **88**: 543–549.
8. Gelb MH, Jain MK, Hanel AM, Berg OG. Interfacial enzymology of glycerolipid hydrolases: lessons from secreted phospholipases A_2. *Annu. Rev. Biochem.* 1995; **64**: 653–688.
9. Gelb MH, Cho W, Wilton DC. Interfacial binding of secreted phospholipases A_2: more than electrostatics and a major role for tryptophan. *Curr. Opin. Struct. Biol.* 1999; **9**: 428–432.
10. Yu BZ, Poi MJ, Ramagopal UA, Jain R, Ramakumar S, Berg OG, Tsai MD, Sekar K, Jain MK. Structural basis of the anionic interface preference and kcat* activation of pancreatic phospholipase A_2. *Biochemistry* 2000; **39**: 12312–12323.
11. Qin S, Pande AH, Nemec KN, He XM, Tatulian SA. Evidence for the regulatory role of the N-terminal helix of secretory phospholipase A_2 from studies on native and chimeric proteins. *J. Biol. Chem.* 2005; **280**: 36773–36783.
12. Qin S, Pande AH, Nemec KN, Tatulian SA. The N-terminal α-helix of pancreatic phospholipase A_2 determines productive-mode orientation of the enzyme at the membrane surface. *J. Mol. Biol.* 2004; **344**: 71–89.
13. Tatulian SA. Structural effects of covalent inhibition of phospholipase A_2 suggest allosteric coupling between membrane binding and catalytic sites. *Biophys. J.* 2003; **84**: 1773–1783.
14. Lee C, Park DW, Lee J, Lee TI, Kim YJ, Lee YS, Baek SH. Secretory phospholipase A_2 induces apoptosis through TNF-α and cytochrome c-mediated caspase cascade in murine macrophage RAW 264.7 cells. *Eur. J. Pharmacol.* 2006; **536**: 47–53.
15. Chang LS, Lin SR, Chang CC. Identification of Arg-30 as the essential residue for the enzymatic activity of Taiwan cobra phospholipase A_2. *J. Biochem. (Tokyo)* 1998; **124**: 764–768.
16. Yang CC, King K, Sun TP. Chemical modification of lysine and histidine residues in phospholipase A_2 from the venom of *Naja naja atra* (Taiwan cobra). *Toxicon* 1981; **19**: 645–659.
17. Yang CC, Chang LS. Role of the N-terminal region in phospholipase A_2 from *Naja naja atra* (Taiwan cobra) and *Naja nigricollis* (Spitting cobra) venoms. *Toxicon* 1988; **26**: 721–731.
18. Chang LS, Lin SR, Chang CC. The essentiality of calcium ion in the enzymatic activity of Taiwan cobra phospholipase A_2. *J. Protein Chem.* 1996; **15**: 701–707.
19. Chang LS, Lin SR, Chang CC. Probing calcium ion-induced conformational changes of Taiwan cobra phospholipase A_2 by trinitrophenylation of lysine residues. *J. Protein Chem.* 1997; **16**: 51–57.
20. Chang LS, Cheng YC, Chen CP. Modification of Lys-6 and Lys-65 affects the structural stability of Taiwan cobra phospholipase A_2. *Protein J.* 2006; **25**: 127–134.
21. Sumandea M, Das S, Sumandea C, Cho W. Roles of aromatic residues in high interfacial activity of *Naja naja atra* phospholipase A_2. *Biochemistry* 1999; **38**: 16290–16297.
22. Eftink MR, Ghiron CA. Fluorescence quenching studies with proteins. *Anal. Biochem.* 1981; **114**: 199–227.
23. Cooper TM, Woody RW. The effect of conformation on the CD of interacting helices: a theoretical study of tropomyosin. *Biopolymers* 1990; **30**: 657–676.
24. Zhou NE, Kay CM, Hodges RS. Synthetic model proteins. Positional effects of interchain hydrophobic interactions on stability of two-stranded α-helical coiled-coils. *J. Biol. Chem.* 1992; **267**: 2664–2670.

25. Chang LS, Kuo KW, Chang CC. Identification of functional involvement of tryptophan residues in phospholipase A_2 from *Naja naja atra* (Taiwan cobra) snake venom. *Biochim. Biophys. Acta* 1993; **1202**: 216–220.
26. Renetseder R, Dijkstra BW, Huizinga K, Kalk KH, Drenth J. Crystal structure of bovine pancreatic phospholipase A_2 covalently inhibited by *p*-bromophenacyl bromide. *J. Mol. Biol.* 1988; **200**: 181–188.
27. Zhao H, Tang L, Wang X, Zhou Y, Lin Z. Structure of a snake venom phospholipase A_2 modified by *p*-bromophenacyl bromide. *Toxicon* 1998; **36**: 875–886.
28. Shakhman O, Herkert M, Rose C, Humeny A, Becker CM. Induction by β-bungarotoxin of apoptosis in cultured hippocampal neurons is mediated by Ca^{2+}-dependent formation of reactive oxygen species. *J. Neurochem.* 2003; **87**: 598–608.
29. Lambeau G, Barhanin J, Schweitz H, Qar J, Lazdunski M. Identification and properties of very high affinity brain membrane-binding sites for a neurotoxic phospholipase from the taipan venom. *J. Biol. Chem.* 1989; **264**: 11503–11510.
30. Donato NJ, Martin CA, Perez M, Newman RA, Vidal JC, Etcheverry M. Regulation of epidermal growth factor receptor activity by crotoxin, a snake venom phospholipase A_2 toxin. A novel growth inhibitory mechanism. *Biochem. Pharmacol.* 1996; **51**: 1535–1543.
31. Lambeau G, Lazdunski M. Receptors for a growing family of secreted phospholipases A_2. *Trends Pharmacol. Sci.* 1999; **20**: 162–170.
32. Yamazaki Y, Matsunaga Y, Nakano Y, Morita T. Identification of vascular endothelial growth factor receptor-binding protein in the venom of eastern cottonmouth – A new role of snake venom myotoxic Lys49-phospholipase A_2. *J. Biol. Chem.* 2005; **280**: 29989–29992.
33. Ponce-Soto LA, Lomonte B, Gutierrez JM, Rodrigues-Simioni L, Novello JC, Marangoni S. Structural and functional properties of BaTX, a new Lys49 phospholipase A_2 homologue isolated from the venom of the snake *Bothrops alternatus*. *Biochim. Biophys. Acta* 2007; **1770**: 585–593.
34. Rouault M, Rash LD, Escoubas P, Boilard E, Bollinger J, Lomonte B, Maurin T, Guillaume C, Canaan S, Deregnaucourt C, Schrevel J, Doglio A, Gutierrez JM, Lazdunski M, Gelb MH, Lambeau G. Neurotoxicity and other pharmacological activities of the snake venom phospholipase A_2 OS2: the *N*-terminal region is more important than enzymatic activity. *Biochemistry* 2006; **45**: 5800–5816.

DOI: 10.1002/psc